Ions at hydrophobic interfaces

2014 J. Phys.: Condens. Matter 26 203101

(http://iopscience.iop.org/0953-8984/26/20/203101)

IOP Publishing Journal of Physics: Condensed Matter

J. Phys.: Condens. Matter **26** (2014) 203101 (11pp) doi:10.1088/0953-8984/26/20/203101

Topical Review

Ions at hydrophobic interfaces

Yan Levin[1] **and Alexandre P dos Santos**[2]

[1] Instituto de Física, Universidade Federal do Rio Grande do Sul, Caixa Postal 15051, CEP 91501-970, Porto Alegre, RS, Brazil
[2] Departamento de Física, Universidade Federal de Santa Catarina, 88040-900, Florianópolis, Santa Catarina, Brazil

E-mail: levin@if.ufrgs.br and alexandre.pereira@ufrgs.br

Received 13 January 2014, revised 28 February 2014
Accepted for publication 3 March 2014
Published 25 April 2014

Abstract

We review the present understanding of the behavior of ions at the air–water and oil–water interfaces. We argue that while the alkali metal cations remain strongly hydrated and are repelled from the hydrophobic surfaces, the anions must be classified into kosmotropes and chaotropes. The kosmotropes remain strongly hydrated in the vicinity of a hydrophobic surface, while the chaotropes lose their hydration shell and can become adsorbed to the interface. The mechanism of adsorption is still a subject of debate. Here, we argue that there are two driving forces for anionic adsorption: the hydrophobic cavitational energy and the interfacial electrostatic surface potential of water. While the cavitational contribution to ionic adsorption is now well accepted, the role of the electrostatic surface potential is much less clear. The difficulty is that even the sign of this potential is a subject of debate, with the *ab initio* and the classical force field simulations predicting electrostatic surface potentials of opposite sign. In this paper, we will argue that the strong anionic adsorption found in the polarizable force field simulations is the result of the artificial electrostatic surface potential present in the classical water models. We will show that if the adsorption of anions were as large as predicted by the polarizable force field simulations, the excess surface tension of the NaI solution would be strongly negative, contrary to the experimental measurements. While the large polarizability of heavy halides is a fundamental property and must be included in realistic modeling of the electrolyte solutions, we argue that the point charge water models, studied so far, are incompatible with the polarizable ionic force fields when the translational symmetry is broken. The goal for the future should be the development of water models with very low electrostatic surface potential. We believe that such water models will be compatible with the polarizable force fields, which can then be used to study the interaction of ions with hydrophobic surfaces and proteins.

Keywords: surface tension, electrolyte, polarizable force fields, ions, dispersion forces

(Some figures may appear in colour only in the online journal)

1. Introduction

Availability of highly reactive halogen ions at the surface of aerosols has tremendous implications for atmospheric chemistry [1–3]. Yet, neither simulations, experiments, nor existing theories are able to provide a fully consistent description of the electrolyte–air interface. The state of the art simulations can be divided into two categories: classical polarizable force field molecular dynamics (PFFMD) [4–11] and *ab initio* quantum density functional theory (DFT) [12–15] simulations. Both of these simulation methods find that large strongly polarizable halide anions, such as bromide and iodide, can become adsorbed at the air–water interface. In fact, classical force fields predict a very strong adsorption of I^- at the interface. If the degree of adsorption were as large as predicted by the classical simulations, the addition of NaI to water would lead to a lowering of

the surface tension of the air–water interface, similar to what happens in solutions containing surfactants. This, however, is not what is found experimentally. The addition of salt to water increases the surface tension of the air–water interface [16, 17]. Presently, available computational resources do not allow for large scale *ab initio* simulations. Nevertheless, it is now possible to simulate a water slab containing about 200 water molecules and one iodide ion. The *ab initio* simulations can be used to calculate the potential of mean force (PMF) for the interaction of I^- with the interface. This potential is significantly less attractive than the one obtained in the classical simulations [18]. The PMF calculated using quantum DFT [19] was found to be in almost quantitative agreement with the recently introduced polarizable anion dielectric continuum theory (PA-DCT) [20, 21]. In this review, we will explore the mechanisms which drive the adsorption of highly polarizable ions to the air–water interface and to other hydrophobic surfaces. We will use the PA-DCT to show that the strong adsorption found using PFFMD simulations arises from the artificial electrostatic surface potential present in the classical water models. The geometry of these models leads to a surface dipole layer—the interfacial water molecules are oriented so that one of the partially charged hydrogens sticks out into the air. This results in an electrostatic potential drop of approximately 600 mV across the air–water interface, with air being more electropositive than water [22, 23]. On the other hand, the *ab initio* simulations find a potential drop of the opposite sign—quantum mechanics predicts that the electronic clouds of water molecules spill out into the air, making air more electronegative than bulk water. We will argue that the artificial surface potential produced by the classical water models is the driving force behind the excessive anionic adsorption found using PFFMD simulations. Therefore, unless these models are modified to remove the artificial surface potential, they cannot be used to study ions at the air–water interface or any other hydrophobic surface.

2. Hydrophobic interfaces

The study of electrolytes at aqueous interfaces is a classical problem of physical chemistry, going back over a century to the pioneering works of Gibbs, Langmuir [24], Wagner [25], and Onsager and Samaras [26]. In spite of this long and venerable history, the interaction of ions with hydrophobic interfaces is still poorly understood and remains a subject of great debate [18, 27–31]. The behavior of ions at interfaces is of great practical importance in such diverse fields as atmospheric chemistry, electrochemistry, colloidal science, biophysics, and physical chemistry. In the case of atmospheric chemistry, it is important to know how ions are distributed inside sea-salt aerosols, since the presence of highly reactive halogens at the surface of microscopic water droplets can lead to production of acid rain and the destruction of tropospheric ozone [1–3]. Adsorption of ions to hydrophobic residues can lead to denaturation of proteins and can affect colloidal stability. Over a hundred years ago, Hofmeister observed that there is a significant degree of specificity in the interaction of ions with proteins—while the addition of some salts can lead to precipitation of protein solutions, other ions can make solutions more stable. The effect of salt on proteins is much more sensitive to anion than to cation. The Hofmeister (lyotropic) series has now been observed in many different systems and has been found to affect micellar formation [32–37], bacterial growth [38], ionic liquids [39, 40], liquid crystals [41, 42], microemulsions [43], critical coagulation concentrations of colloidal suspensions [44–49], etc. Over a century ago [50], the lyotropic series was also observed in the surface tension measurements of electrolyte solutions [16, 17, 51, 52]. An explanation for why salts increase the surface tension of the air–water interface was provided by Wagner [25] and Onsager and Samaras [26] (WOS), who argued that as an ion approaches a dielectric interface, it induces a surface charge which repels it from the interface. On the basis of the Gibbs adsorption isotherm equation WOS then argued that ionic depletion from the interfacial region will result in increased surface tension. Contrary to this explanation, however, recent photoelectron-spectroscopy measurements [53–56] have shown that some anions can be present at the air–water interface. Subsequently, atomistic molecular dynamics simulations [4–11] and quantum *ab initio* simulations [12–15] have confirmed that some polarizable anions might be adsorbed to the air–water interface. The ionic propensity for hydrophobic surfaces was, once again, found to follow the Hofmeister series [57–59], showing that WOS theory is incomplete. Dispersion interactions, neglected in the WOS approach, were suggested to be responsible for the ionic specificity [60]. It was soon realized, however, that although the dispersion forces are important for the interaction of ions with the hydrophobic surfaces, they can not explain the propensity of large halogen anions for the air–water interface—the dispersion interactions favor the adsorption of small weakly polarizable cations and not of strongly polarizable anions [61].

Recently, a new theory was developed which allows us to calculate the surface tensions for different electrolytes at various hydrophobic interfaces [20, 21, 62–64]. The results of the theory are in excellent agreement with the experiments. The theory shows that while the alkali metal cations remain strongly hydrated and are repelled from the hydrophobic surfaces, the anions belong to two categories: kosmotropes and chaotropes. The structure-making kosmotropes remain strongly hydrated in the vicinity of a hydrophobic surface, while the structure-breaking chaotropes lose their hydration shell and can become adsorbed to the interface. It is important to stress that, in this theory, the notion of kosmotropes and chaotropes has nothing to do with the long-range influence of ions on the hydrogen bond network of water: instead, it only refers to the local ionic hydration. The theory allows us to explore in great detail the various driving forces responsible for the ionic adsorption to hydrophobic surfaces. The interaction potentials predicted by the theory can be compared with the PMF obtained using the explicit-water molecular dynamics simulations, and the effect of the ion-interface interaction on the thermodynamic properties of the electrolyte solution—such as its surface tension—can be easily calculated.

At the moment, there is an intense debate on the role of the interfacial electrostatic surface potential of water on ionic adsorption [65, 66]. The classical point charge water models predict a surface potential of a neat air–water interface to be

approximately −600 mV [22, 23], while the potential obtained using *ab initio* quantum DFT simulations is of the opposite sign and is significantly larger, +3000 mV [13, 14]. Nevertheless, when properly coarse grained, the surface potential of *ab initio* simulations vanishes, while the classical surface potential persists [67]. In this paper, we will show that the electrostatic surface potential of the extended simple point charge model (SPC/E) of water is partially responsible for the excessive adsorption predicted by the polarizable force field simulations. Furthermore, we will show that if the adsorption of anions is as strong as predicted by these simulations, the excess surface tension of NaI would be strongly negative, instead of positive, as measured experimentally. Below we will review the PA-DCT and explore the contributions of cavitation, polarizability, dispersion and the electrostatic surface potential on ion-interface interaction.

3. Theory: water–air interface

We first briefly review the interaction potential between an ion and the air–water interface [20, 21, 62]. The potential is constructed by taking into account the polarization, hydration, cavitation and image charges. This potential will then be used in a modified Poisson–Boltzmann (PB) equation to calculate the ionic density distribution near an interface.

The standard model of electrolyte solutions treats ions as hard spheres with a point charge located at the center. This is the basis of the celebrated Debye–Hückel (DH) [68] theory. This theory, and its subsequent extensions, such as the Mean Spherical Approximation (MSA) and the Hypernetted Chain equation (HNC), have been found to be very accurate for describing the bulk properties of electrolyte solutions [69]. On the other hand, the rigid charge distribution of the DH and Onsager and Samaras [26] theories does not permit ionic presence at the air–water interface. The reason for this is that the electrostatic self-energy penalty for exposing the rigid ionic charge to the low dielectric environment overwhelms any other entropic or enthalpic gain in free energy that arises from the surface solvation [70]. Ionic polarizability appears to be the key ingredient necessary to understand ionic adsorption at the hydrophobic interfaces [20]. Polarizable ions can shift their electronic charge density so that it remains mostly hydrated by the water molecules of the topmost interfacial layer. Large polarizability decreases dramatically the self-energy penalty of surface solvation.

A polarizable ion can be modeled as an imperfect spherical conductor of relative polarizability $\alpha = \gamma_i/a^3$, where γ_i is the ionic polarizability. Note that for a perfect conductor $\alpha = 1$. The electrostatic self energy of an ion at distance z from the interface can be written as [20]

$$\beta U_p(z;x) = \begin{cases} \dfrac{\lambda_B}{2a} & \text{for } z \geq a\,, \\ \dfrac{\lambda_B}{2a}\left[\dfrac{\pi x^2}{\theta(z)} + \dfrac{\pi(1-x)^2\,\epsilon_w}{[\pi-\theta(z)]\epsilon_o}\right] + & \\ g\left[x - \dfrac{1-\cos[\theta(z)]}{2}\right]^2 & \text{for } -a < z < a\,, \end{cases} \tag{1}$$

where $\lambda_B = \beta\, q^2/\epsilon_w$ is the Bjerrum length, 7.2 Å for water at room temperature, $g = (1-\alpha)/\alpha$, $\theta(z) = \arccos(-z/a)$ and x is the fraction of the ionic charge that remains hydrated. Minimizing equation (1), we obtain the expression for $x(z)$,

$$x(z) = \frac{\frac{\lambda_B \pi \epsilon_w}{a\epsilon_o[\pi-\theta(z)]} + g[1-\cos[\theta(z)]]}{\frac{\lambda_B \pi}{a\theta(z)} + \frac{\lambda_B \pi \epsilon_w}{a\epsilon_o[\pi-\theta(z)]} + 2g}\,. \tag{2}$$

Inserting this expression into equation (1) yields the electrostatic self energy of an ion at distance z from the interface, $U_p(z)$. We find that the self energy of a polarizable ion located at the interface is an order of magnitude smaller than the energy of a hard non-polarizable ion at the same position [70]. From the electrostatic perspective, therefore, polarizable ions will still prefer bulk solvation.

What then drives polarizable ions towards the interface? To solvate an ion requires the creation of a cavity into which the ion is inserted. It is clear that any perturbation to the hydrogen bond network of water costs energy which, for small cavities, is predominantly entropic and scales with the volume of the cavity. Clearly, if an ion is expelled from water this will result in a cavitational free energy gain. We will, therefore, suppose that the cavitational free energy is proportional to the ionic volume exposed to the aqueous medium [20, 71]. The cavitation potential can then be written as

$$\beta U_c(z) = \begin{cases} \nu a^3 & \text{for } z \geq a\,, \\ \dfrac{1}{4}\,\nu a^3 \left(\dfrac{z}{a}+1\right)^2 \left(2-\dfrac{z}{a}\right) & \text{for } -a < z < a\,, \end{cases} \tag{3}$$

where $\nu = 0.3$ Å^3 is obtained using SPC/E water simulations [71].

The broken translational symmetry, imposed by the air–water interface, leads to two additional contributions to the free energy of the ion-interface interaction. As the ion approaches the interface, the spherically symmetric screening of its electric field is perturbed, resulting in higher electrostatic energy. The dielectric discontinuity also results in the build-up of the surface charge: both of these effects lead to the repulsion of the ion from the interface. Effects of the dielectric discontinuity in ionic solutions have been extensively studied over the last decade [72–76]. The energy cost to bring an ion from bulk water to a distance z from the air–water interface was calculated by Levin and Flores-Mena [73]. The Levin–Flores-Mena potential can be well approximated by [62, 77]

$$\beta U_i(z) = \begin{cases} \beta W a \dfrac{e^{-2\kappa(z-a)}}{z} & \text{for } z \geq a\,, \\ \beta W \dfrac{z}{a} & \text{for } 0 \leq z < a\,, \\ 0 & \text{for } -a \leq z < 0\,, \end{cases} \tag{4}$$

where $\kappa = \sqrt{8\pi\lambda_B c_s}$ is the inverse Debye length. The potential at contact, W, is given by [77],

$$\beta W = \frac{\lambda_B}{2}\int_0^\infty \mathrm{d}\,k\,\frac{k\,f_1(k)}{p\,f_2(k)}\,, \tag{5}$$

where

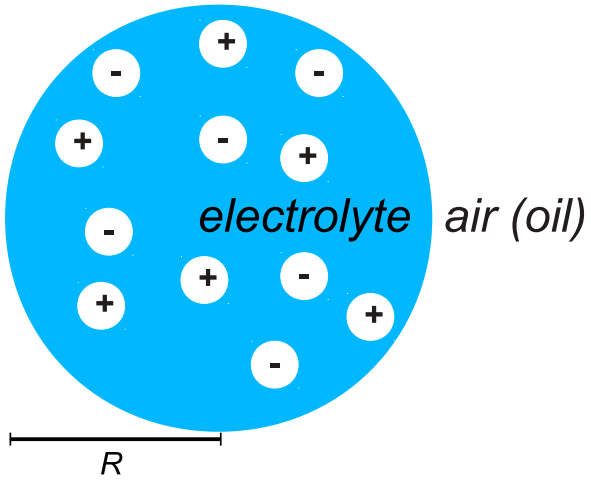

Figure 1. Illustration of the spherical drop model.

$$f_1(k) = p\,\cosh(ka) - k\,\sinh(ka) + \frac{\epsilon_o}{\epsilon_w} p\,\sinh(ka) - \frac{\epsilon_o}{\epsilon_w} k\,\cosh(ka)\,,$$

$$f_2(k) = p\,\cosh(ka) + k\,\sinh(ka) + \frac{\epsilon_o}{\epsilon_w} p\,\sinh(ka) + \frac{\epsilon_o}{\epsilon_w} k\,\cosh(ka)\,,$$

and $p = \sqrt{k^2 + \kappa^2}$.

A somewhat different approach for calculating the ion-interface surface potential has been recently proposed by Wang and Wang [78]. For the air–water or oil–water interfaces, the two models lead to very similar interaction potentials.

4. Surface tension: the drop model

The ion-interface interaction potentials derived in the previous section can be used to calculate the excess surface tension of an electrolyte–air interface. Consider cations and anions of radii a inside a water drop of radius R: see figure 1. For simplicity of notation, we use the same letter a to denote the radii of all ions, note, however, that the numerical value of a will be different for each ion. Furthermore, while for kosmotropes a is the hydrated radius [79], for chaotropes it is the crystallographic (Latimer) radius [80]. The chaotropic ions can cross the interface up to the maximum distance $r_m = R+a$ from the center of the drop. We do not need to consider larger distances, since the growing self energy makes it very improbable for an ion to move farther than this into the low dielectric phase. The kosmotropic ions remain strongly hydrated and reach, at most, the distance $r_m = R - a$ from the center of the drop. The drop is taken to be sufficiently large, R = 300 Å, so that the curvature effects can be neglected.

The interfacial tension is calculated using the Gibbs adsorption (GA) isotherm equation,

$$d\gamma = -\Gamma_+ d\mu_+ - \Gamma_- d\mu_-\,, \tag{6}$$

where $\Gamma_\pm = [N - V\,\rho_\pm(0)]/S$ is the ionic excess, $\mu_\pm$ are the chemical potentials, N is the number of cations or anions, $\rho_\pm(0)$ are the bulk concentrations, and S and V are the surface and the volume of the drop, respectively. The bulk concentrations are obtained from the numerical solution, in spherical coordinates, of the modified (PB) equation:

$$\nabla^2\phi(r) = -\frac{4\pi q}{\epsilon_w}\left[\rho_+(r) - \rho_-(r)\right],$$

$$\rho_\pm(r) = A_\pm e^{\mp\beta q\phi(r) - \beta U_\pm(r)}\,, \tag{7}$$

$$A_\pm = N\left[4\pi\int_0^{r_m} d\,r\,r^2 e^{\mp\beta q\phi(r) - \beta U_\pm(r)}\right]^{-1},$$

where r is the distance from the center of the drop, q is the proton charge, $\phi(r)$ is the electrostatic potential with $\phi\,(0) = 0$ and $\phi'(0) = 0$, and $\rho_\pm(r)$ are the ionic density profiles. At the level of PB theory, correlations between the ions are ignored, which has been found to be a very reasonable approximation for 1 : 1 aqueous electrolytes with concentrations up to 1 M, as considered in this paper [81, 82]. The ionic chemical potentials, $\beta\mu_\pm = \log[\Lambda_\pm^3\rho_\pm(0)]$, are uniform throughout the drop, where $\Lambda_\pm$ are the thermal de Broglie wavelengths. The Gibbs dividing surface (GDS) is defined at $r = R$. The GDS separates the aqueous and the vapor mediums, modeled as continuum uniform dielectrics with constants ϵ_w and ϵ_o, respectively. The heterogeneity of the dielectric constants is taken into account by the ion-interface interaction potentials, $U_\pm(r)$, discussed in the previous section and defined later in the text.

With the ionic potentials in hand, we can solve the PB equation, equation (7), iteratively and calculate the excess surface tensions of various electrolyte solutions, equation (6). For halides, the separation of ions into kosmotropes and chaotropes has been found to be very strongly correlated with their crystallographic radii—small halogen ions, such as F^- and Cl^-, produce very intense electric fields which interact strongly with the surrounding water molecules leading to formation of ion-water complexes. On the other hand, in the vicinity of a fluctuating interface, a relatively weak electric field of large halides is not sufficient to keep water molecules bound to them, so that chaotropes can become 'dehydrated'. Unfortunately, for polyatomic anions, there is no simple correlation between either ionic size or ionic polarizability and the ionic hydration. However, we find that there is an excellent correlation [62] between the Jones–Dole (JD) viscosity B coefficient [83, 84] and ionic hydration near a hydrophobic interface. The JD B coefficient is obtained from a phenomenological fit of the excess viscosity produced by the addition of salt to water,

$$\eta_r = 1 + A\sqrt{c} + Bc\,, \tag{8}$$

where η_r is the relative viscosity, c is the concentration of electrolyte, and A and B are the fitting parameters, obtained experimentally. The coefficient A is due to the relaxation of the ionic atmosphere perturbed by the shear flow which, for small concentrations, can be calculated using the Debye–Hückel–Onsager–Falkenhagen theory [85]. On the other hand, the B coefficient depends on the microscopic ion-solvent interaction. For structure-making ions (kosmotropes), the B coefficient is positive, while for structure-breaking ions (chaotropes) it is

Table 1. Ion classification into chaotropes (c) and kosmotropes (k). Effective radii (hydrated or partially hydrated) for kosmotropes and (bare) for chaotropes. For chaotropes we have also included the ionic polarizabilities, which are irrelevant for kosmotropes. The polarizabilities are taken from [87], the bare radii from [80] and the hydrated radii from [79].

Ions	chao/kosmo	radius (Å)	polarizability (Å^3)
F^-	k	3.52	—
Cl^-	k	2	—
Br^-	c	2.05	5.07
I^-	c	2.26	7.4
IO_3^-	k	3.74	—
BrO_3^-	k	2.41	—
NO_3^-	c	1.98	4.09
ClO_3^-	c	2.16	5.3
ClO_4^-	c	2.83	5.45
CO_3^{-2}	k	3.94	—
SO_4^{-2}	k	3.79	—

negative. It is curious that a dynamical property, such as viscosity, is found to be so strongly correlated with a static property, such as the interfacial tension of the interface. The reason for this correlation might be that the strong fluctuations of the instantaneous interface can strip the weakly bound water molecules from a chaotropic ion, similar to what happens in a shear flow. Unfortunately, at the moment, there is no quantitative theory of ionic hydration, for which quantum effects seem to be important. To understand the difficulties involved, consider the iodate ion, IO^-_3. This ion is very large and strongly polarizable (polarizability of 8 Å^3). On the other hand, its positive viscosity B coefficient, see table 1, classifies it as a kosmotrope. In spite of its large size and polarizability it should, therefore, remain strongly hydrated near the air–water interface. This should be contrasted with the smaller and less strongly polarizable iodide, I^-, which is a chaotrope and must lose its hydration sheath near a hydrophobic surface. It is impossible to understand this dichotomy simply on the basis of ionic size and polarizability, both of which suggest that IO^-_3 should be an excellent chaotrope. The recent *ab initio* simulations [86] show a very curious electronic structure of IO^-_3, which might explain the peculiar hydration properties of iodate. In the absence of a theory of ionic hydration we will, therefore, adopt the viscosity B coefficient as an indicator of kosmotropic/chaotropic ionic classification. Since kosmotropes remain hydrated, for these ions we will impose a hard-core repulsion at one hydrated radius from the interface. On the other hand, the chaotropes lose their hydration sheath, so that for these ions we will need their bare radii as an input for our theory. The hydrated radii are taken from Nightingale [79] and the bare radii from Latimer *et al* [80]. In table 1, we summarize the ionic classification and the parameters used in the potentials.

The anion-interface interaction potentials are $U_-(z) = U_i(z)$ for kosmotropes, and $U_-(z) = U_p(z)+U_c(z)+U_i(z)$ for chaotropes. The potential for cation Na^+, which is also a kosmotrope, is $U_+(z) = U_i(z)$. Note that z is the distance from the interface, while r, in the PB equation, is the distance from the center of the drop. Starting with a NaI solution, we adjust the ionic hydration radius of Na^+ to obtain the best fit of the experimental surface tension data, see figure 2. We find that $a = 2.5$ Å results in an excellent agreement with experiment.

The same ionic radius of Na^+ is then used to calculate the surface tensions of all other sodium salts. We see that the theory agrees very well with all the experimental data, except for $NaClO_4$, see figure 2. The deviation from the experimental data, in this case, might be due to an overestimate of the effective radius of ClO^-_4. Since the cavitational energy scales with the cube of the ionic radius, a small error can result in a significant overestimate of ionic adsorption. An excellent agreement between the theory and experiment for $NaIO_3$ shows that, in spite of its huge size and large polarizability, iodate remains strongly hydrated and is repelled from the air–water interface.

The theory can also be used to calculate the excess electrostatic potential difference across the air–water interface, resulting from the preferential anion adsorption, $\Delta\phi = \phi(\infty)-\phi(0)$. Frumkin [90] was the first to measure a negative value of $\Delta\phi$, showing that there is some partitioning of ions across the interface. In table 2, we present the theoretical results for the excess electrostatic potentials of various 1 M electrolyte solutions and compare them with the experimental measurements of Frumkin [90] and Jarvis and Scheiman [91]. In spite of a large scatter in the experimental data, there is a reasonable qualitative agreement between the theory and experiments.

The ion-interface interaction potential for I^- calculated using the PA-DCT theory, $U_-(z) = U_p(z)+U_c(z)+U_i(z)$, and the PMFs calculated using the PFFMD and the *ab initio* DFT simulations are plotted in panel (*a*) of figure 3. The agreement between the interaction potential calculated using the PA-DCT theory and the PMF of the *ab initio* simulation is evident. On the other hand, the PMF of a classical PFFMD simulation has a potential well of ≈3 k_BT, significantly larger than what is seen in the *ab initio* simulation. In the following section we will explore the origin of this discrepancy.

5. Surface potential of water

The PA-DCT theory shows an excellent agreement with the experimental measurements of surface tensions of various electrolyte solutions, with only one adjustable parameter, the radius of Na^+. This suggests that the ion-interface interaction potentials predicted by this theory are quite accurate. Yet, when compared with the PMF of I^- calculated using PFFMD simulations, there is a dramatic difference, see panel (*a*) of figure 3.

While the PA-DCT predicts only a small metastable minimum for I^- adsorption at the air–water interface, the PFFMD finds a global minimum of almost 3 k_BT deep! Clearly, existence of such strong attractive interaction between I^- and the interface would result in a strong adsorption. Indeed, as we will show later, if the adsorption were as strong as predicted by the PFFMD, the excess surface tension of the NaI solution would be strongly negative, contrary to the experimental measurements. Furthermore, in agreement with the PA-DCT and contrary to PFFMD, the quantum DFT *ab initio* simulations also find only a small metastable minimum for the PMF of I^-. The question of fundamental importance is then: What produces such strong attraction between anions and the air–water interface in the PFFMD? The huge number of parameters in classical water and ion models makes it very

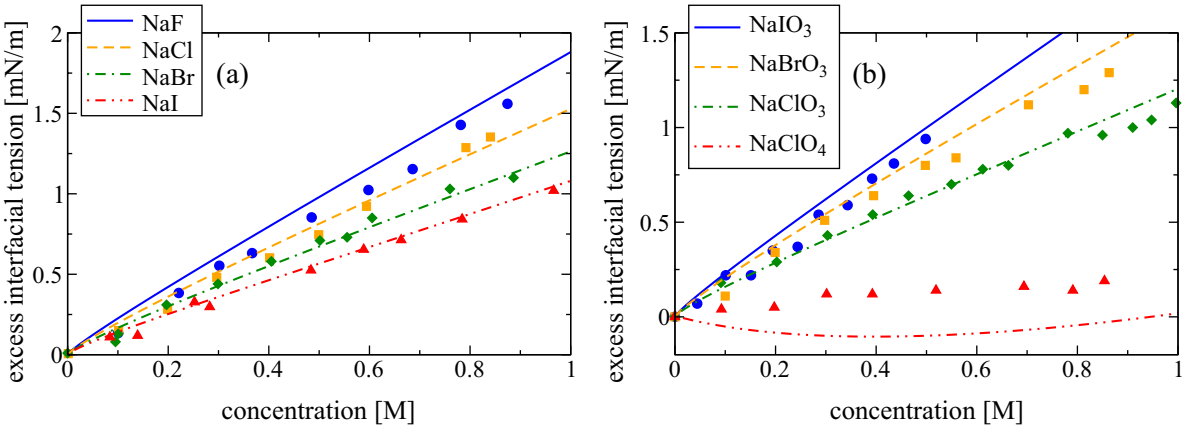

Figure 2. Excess interfacial tensions as a function of salt concentration. The theory is represented by the lines, while the symbols are the experimental data [17, 88, 89]. In panel (*a*) the circles, squares, diamonds, and triangles represent the experimental data for salts NaF, NaCl, NaBr and NaI, respectively. In panel (*b*) the circles, squares, diamonds, and triangles represent the experimental data for salts $NaIO_3$, $NaBrO_3$, $NaClO_3$ and $NaClO_4$, respectively.

Table 2. Experimental and calculated electrostatic surface potential differences for 1 M electrolytes.

Salts	Calculated (mV)	[90, 92] (mV)	[91] (mV)
NaF	4.7	—	—
NaCl	−2.1	−1	≈ −1
NaBr	−9.4	—	≈ −5
NaI	−14.3	−39	≈ −21
$NaIO_3$	5	—	—
$NaBrO_3$	−0.12	—	—
$NaNO_3$	−8.27	−17	≈ −8
$NaClO_3$	−11.02	−41	—
$NaClO_4$	−31.1	−57	—
Na_2CO_3	10.54	3	≈6
Na_2SO_4	10.17	3	≈35

difficult to untangle the different contributions to free energy and to attribute cause and effect [65]. Here, we will argue that the driving force for the excessive anionic adsorption in PFFMD models comes partially from the artificial electrostatic surface potential. The geometry of the classical point charge water models leads to a dipole layer resulting from a broken translational symmetry. To optimize the hydrogen bond network, the surface water molecules become oriented so that one of the partially charged hydrogens sticks out into the air. This leads to a dipole layer with an excess of positive charge in air and negative charge in water. For the SPC/E water model, the dipole layer results in an electrostatic potential drop of approximately 550 mV across the air–water interface, with air being more electropositive than water [22, 23]. To understand the effect of electrostatic surface potential on ionic adsorption of polarizable ions, we can include this contribution into our PA-DCT. To do this we add to the polarization energy, equation (1) (in the region $-a < z < a$), a contribution due to the interaction of ionic electronic charge with the artificial dipole water layer. Recalling that x is the fraction of the ionic charge that is solvated, the gain in electrostatic energy due to the interaction of an anion with the water dipole-layer is then $q\Delta\chi[1 - x(z)]$, where $\Delta\chi = -550$ mV is the electrostatic surface potential of SPC/E water [22, 23]. In reality a partial cancellation of the surface potential across the air–water and the solute–water interface [93] will probably lower the value of the effective surface potential [66]. However, since it is not clear what this cancellation will be for polarizable ions, for the purposes of the present paper we will use the full value of $\Delta\chi$.

The polarization potential, equation (1) (with dipole-layer ion contribution), $U_{p\chi}(z;x)$, must then be minimized to calculate the ionic charge that remains hydrated as the ion moves across the interface, $x(z)$. Substituting $x(z)$ back into $U_{p\chi}(z;x(z))$, we obtain the interaction energy of an ion with the dielectric dipole-layer interface. To make a direct comparison with the PFFMD, we need to make a few additional modifications. Unlike the real water with relative dielectric permittivity of 80, SPC/E water has a dielectric constant of about 69 [66, 94]. Furthermore, unlike the ions of PA-DCT, ions of PFFMD are not hard spheres, so there is no simple mapping between the radii used in PA-DCT and the Lennard–Jones parameters of the PFFMD. Our strategy will then be to adjust the effective 'hard-core' radius of the iodide ion to get the same adsorption as found in the PFFMD simulations [8].

To compare with PFFMD, we solve the PB equation, equation (7), in the slab geometry, with the modified potential, $U_{-}(z) = U_{p\chi}(z)+U_{i}(z)+U_{c}(z)$. The concentration of NaI is taken to be 1.2 M, the same as used in PFFMD [8]. The Bjerrum length is modified to $\lambda_B = 8.34$ Å, to account for the reduced dielectric constant of SPC/E water.

We find that to get the same adsorption of iodide, as seen in PFFMD, using our dipole-layer modified PA-DCT, the hard-core radius of I^- must be changed to $a = 2.9$ Å, instead of the Latimer radius of $a = 2.26$ Å, see figure 4. However, after this modification, the density profiles both of Na^+ and I^- become very similar to the ones observed in the PFFMD simulations. We note, however, that due to the hard-core repulsion from the interface imposed by the PA-DCT on the kosmotropic ions, our model predicts slightly less adsorption of sodium than is found in PFFMD simulations. Integrating the Gibbs adsorption isotherm equation, we can now calculate the excess surface tension of the NaI solution. As expected, the excess surface tension of the dipole-layer modified PA-DCT is strongly negative, contrary to the experimental data, see

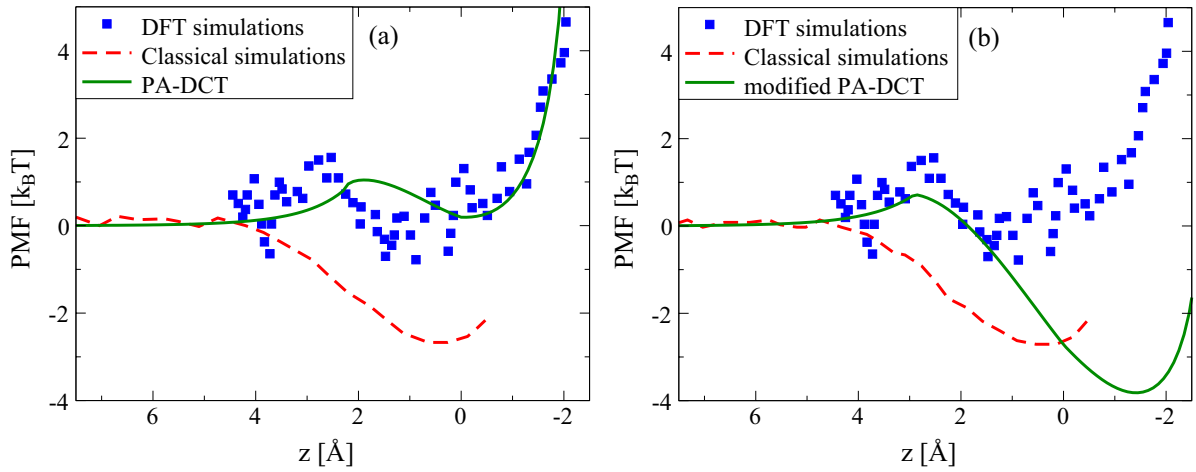

Figure 3. Comparison between the ion-interface interaction potentials obtained from the pure and dipole-layer modified PA-DCT, and the PMFs calculated using DFT *ab initio* and the classical PFFMD simulations. In panel (*a*), the comparison is with the pure PA-DCT theory, in panel (*b*), with the dipole-layer modified PA-DCT one. The simulation data are taken from [18]

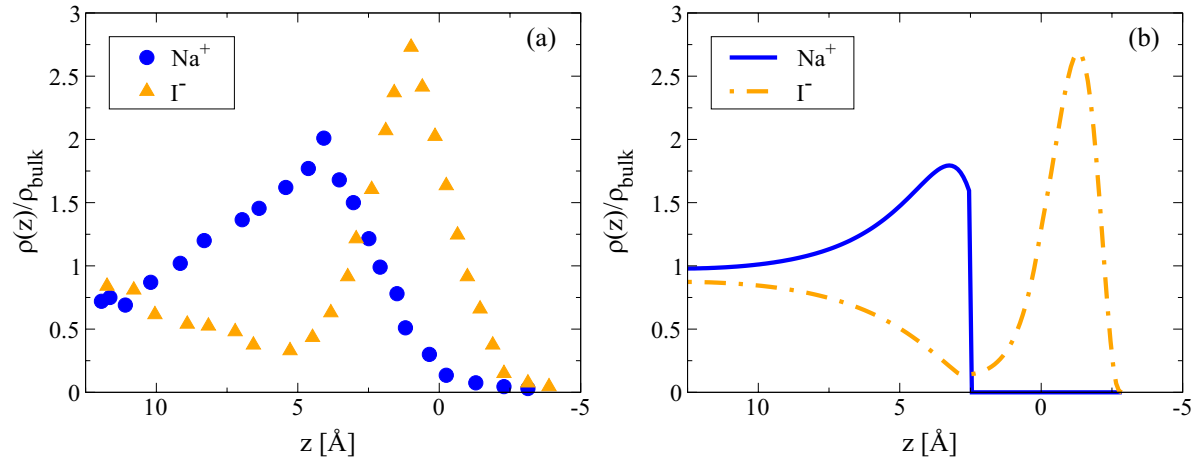

Figure 4. Comparison between the density profiles obtained using PFFMD simulations (symbols) and the dipole-layer modified PA-DCT (lines), for the NaI salt. The simulation data are obtained from figure 10 of [8].

figure 5. It is important to stress that, because of a stronger adsorption of Na^+ observed in PFFMD simulations, see figure 4, the surface tension of NaI in classical point charge water models [95] will be even lower (more negative) than is predicted by the dipole-layer modified PA-DCT. This is clearly incorrect, which shows that there is a fundamental incompatibility of polarizable ionic force fields with the currently used point charge water models.

In panel (*b*) of figure 3, we show the comparison of the ion-interface interaction potential calculated using the dipole-layer modified PA-DCT and the PMF calculated using PFFMD simulations. The two potentials are very similar, although the theoretical result has a slightly larger minimum and is shifted more towards the vapor phase. The discrepancy might be due to the fact that the PMF of the simulations is plotted with respect to the GDS and not with respect to the instantaneous interface [96]. Indeed, when the simulation PMF is replotted with respect to the instantaneous interface [97], the two potentials become very similar.

The PA-DCT theory has been shown to accurately predict the surface tensions of electrolyte solutions. It has also provided us with a valuable insight into the origin of the excessive anionic adsorption observed in PFFMD simulations. In the following sections, we will use the PA-DCT to study the surface tensions of acids [63] and the interfacial tensions of electrolyte–oil interfaces [64].

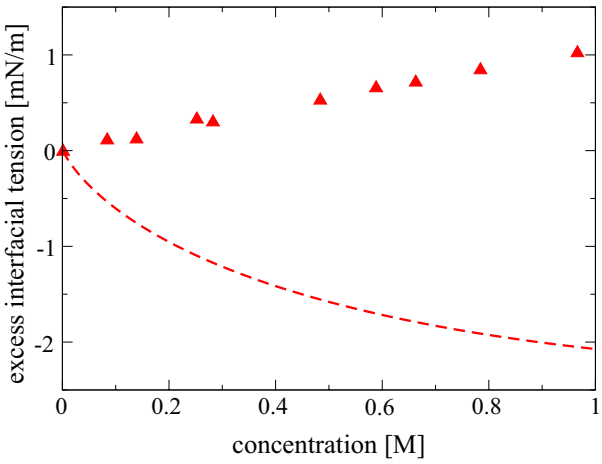

Figure 5. Excess interfacial tension as a function of salt concentration for NaI salt. The dipole-layer modified PA-DCT is represented by the line, while symbols are the experimental data.

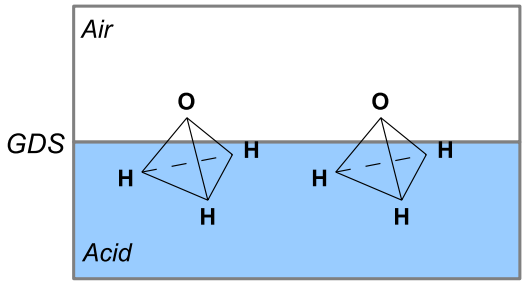

Figure 6. Illustration of hydronium ions adsorbed at the acid–air interface. Observe the preferential orientation of hydronium.

6. Acid solutions

Unlike salts, the addition of most acids to water causes a decrease of the surface tension of the solution–air interface [16, 98]. It is well known that a proton of H^+ interacts strongly with water molecules, resulting in the formation of complexes [99–101] such as H_3O^+ and $H_2O_5^+$. In particular, the hydronium ion, H_3O^+, has a pyramidal trigonal structure with hydrogens at the base and oxygen at the top [102]. In this geometry, oxygen is a bad hydrogen bond receptor, while hydrogens are good hydrogen bonds donors [103], providing an amphiphilic character to H_3O^+ behavior [104, 105], see figure 6.

Quantum *ab initio* simulations [103, 106], experiments [105], and classical simulations [102] all indicate large surface activity of hydronium ion. It is straightforward to modify the PA-DCT to explore the thermodynamics of acid solutions. The amphiphilic character of hydronium results in a strong adsorption of this ion at the air–water interface. The interaction of hydronium with the interface can be modeled by an attractive square well potential. The range of the potential is taken to be one hydrogen bond length, 1.97 Å, from the interface. The depth of the potential is then adjusted to fit the surface tensions of one of the electrolyte solutions, i.e. HCl, see figure 7. The same hydronium-interface potential is then used to calculate the surface tensions of all other acids. For ions, the interaction potentials are the same as the ones used in the previous sections of this review.

The ionic and hydronium density profiles are calculated by solving the modified PB equation, equation (7), with the hydronium potential given by $U_+(z) = U_h(z)+U_i(z)$, where $U_h(z)$ is the square well potential and $U_i(z)$ is the charge-image interaction potential with zero radius, $a = 0$. The excess surface tension of the HCl solution is then calculated by integrating the Gibbs adsorption isotherm, equation (6). We find that if the depth of the square well potential is adjusted to $-3.05\ k_BT$, we obtain an excellent agreement with the experimental surface tensions of the hydrochloric acid, figure 7. The same hydronium potential,

$$\beta U_h(z) = \begin{cases} 0 & \text{for } z \geq 1.97\ \text{Å}, \\ -3.05 & \text{for } 0 \leq z < 1.97\ \text{Å}, \end{cases} \tag{9}$$

is then used to calculate the surface tension of all other acids, figure 7. Although for most acids we find a very good agreement with the experimental measurements, significant deviations are observed for $HClO_4$. This is similar to what has been found for $NaClO_4$ and is, again, attributed to the overestimate of the effective radius of ClO_4^-, quoted in the literature.

7. Water–oil interface

The hydrophobic surfaces are more complicated than the air–water interface. Besides the cavitational energy responsible for the chaotropic adsorption at the air–water interface, we must also consider possible dispersive interactions with the low-dielectric hydrophobic medium. At this time there are no *ab initio* simulations indicating the value of the electrostatic potential difference across the neat water–hydrophobe interface. In the absence of such measurements, we will suppose that, similar to the air–water interface, the electrostatic surface potential is negligible.

To construct a theory of ionic interaction with a hydrophobic surface—which will be modeled as an interface between water and oil—we will follow the same procedure developed for the air-water interface. We will suppose that kosmotropic ions will remain hydrated and will be repelled from the interface, while the chaotropic ions can lose their hydration sheath and become adsorbed at the interface. Since the dielectric constant of oil is very low, we can use the same polarization and charge-image potentials, equations (1) and (4), respectively, developed for the air–water interface. The cavitational energy gain, however, is different for a fluid–fluid interface than for the air–water interface. As the ion moves from water of the oil, it decreases the perturbation of the aqueous environment, while increasing the perturbation to oil. For small cavities, this energy is mostly entropic. The molecular weight of dodecane, used in experiments, is ten times larger than that of water, while its mass density is very similar to water, so that the number of oil molecules excluded from a cavity of radius a is, on average, an order of magnitude smaller than that of water molecules for a cavity of the same radius. This means that the cavitational penalty of creating a hole in oil should be an order of magnitude lower than that for creating a cavity of the same radius in water. Therefore, for high molecular weight oils, the cavitational potential, equation (3), will be the same as for the air–water interface [64].

The dispersion interaction between ions and oil arises from the quantum fluctuations of the electronic clouds. The dispersion interaction is proportional to the ionic polarizability which, in turn, is proportional to the ionic volume. We will, therefore, model the dispersion potential to be proportional to the relative ionic polarizability and to the ionic volume exposed to oil [64],

$$\beta U_d(z) = \begin{cases} 0 & \text{for } z \geq a\ , \\ A_{\text{eff}}\alpha & \\ \left[1 - \dfrac{(z/a+1)^2(2-z/a)}{4}\right] & \text{for } -a < z < a\ , \end{cases} \tag{10}$$

where A_{eff} is the effective Hamaker constant, which can be adjusted to fit the interfacial tension of one of the electroltye solutions.

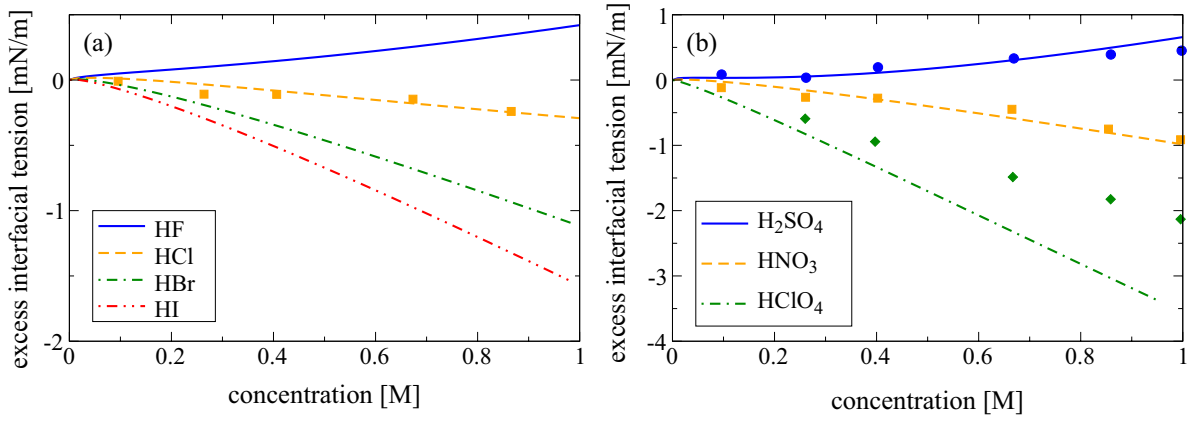

Figure 7. Excess interfacial tension as a function of salt concentration. Our theory is represented by the lines, while the symbols are the experimental data [16]. In panel (*a*) the squares represent experimental data for acid HCl. In panel (*b*) the circles, squares and diamonds represent experimental data for acids H_2SO_4, HNO_3 and $HClO_4$, respectively.

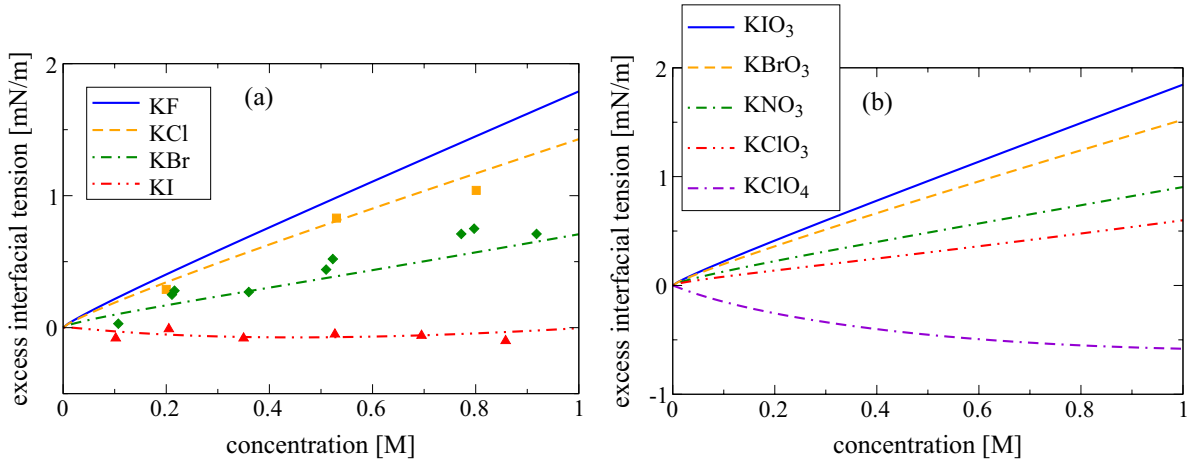

Figure 8. Excess interfacial tension as a function of salt concentration. The theory is represented by the lines, while the symbols are the experimental data [51]. In panel (*a*) the squares, diamonds and triangles represent experimental data for salts KCl, KBr and KI, respectively. There are no experimental data for salts represented in panel (*b*).

We are not aware of experimental data for interfacial tensions of sodium salts. The only data available to us is for potassium salts. Therefore, we must first recalibrate the effective radius of cation. We find that using the hydrated radius of K^+ to be $a = 2$ Å, we obtain a good agreement with the experimental data for KCl, see figure 8. We will use the same radius of K^+ in all other calculations. We next adjusted the value of the effective Hamaker constant. We find that $A_{\text{eff}} = -4$ yields a good fit of the excess interfacial tension of a KI solution, see figure 8. The same value of A_{eff} is then used to calculate the interfacial tensions of other salts containing chaotropic anions, see figure 8. The value of $A_{\text{eff}} = -4$ is surprisingly close to a theoretical estimate [64], $A_{\text{eff}} \approx -4.4$.

In figure 9, we show the ionic density profiles. As expected, the dispersion interaction leads to a significant increase in anionic adsorption at a hydrophobic surface, compared to the air–water interface.

In figure 10, we plot the ion-interface interaction potential of I^-, which now shows a global minimum of about 2 k_BT at the interface. Finally, in table 3, we present the excess electrostatic potential difference across the oil–water interface for various electrolyte solutions at 1 M concentration.

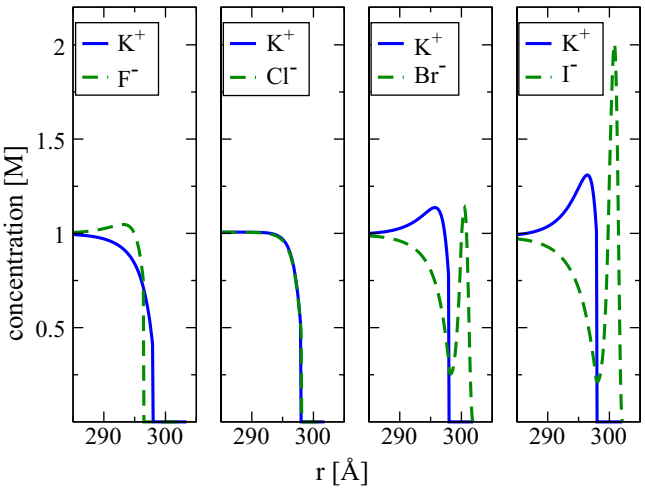

Figure 9. Ionic density profiles for potassium salts at 1 M. The GDS is at $r = 300$ Å.

8. Conclusions

We have used the PA-DCT to explore the interaction of ions with hydrophobic surfaces. The theory shows that ions must

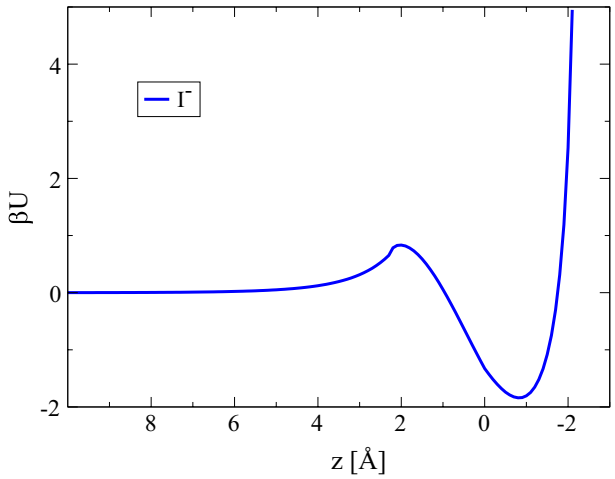

Figure 10. Oil–electrolyte interface interaction potential of I^-, at 1 M.

Table 3. Surface potential differences for various potassium salts at 1 M concentration.

Salt	Calculated (mV)
KF	5.85
KCl	−0.23
KNO_3	−13.18
KBr	−17.45
KI	−30.56

be divided into two classes: structure-making kosmotropes and structure-breaking chaotropes. In the context of the present theory, structure making/breaking does not refer to any long-range influence of ions on water, instead the kosmotropic/chaotropic classification is only used to characterize ionic hydration near a hydrophobic surface. Ions which have positive JD viscosity *B* coefficients and have historically been called structure makers (kosmotropes) are found to remain strongly hydrated near a hydrophobic surface. On the other hand, ions with negative JD viscosity *B* coefficients, structure breakers (chaotropes), are found to lose their hydration sheath and as a result of their large polarizability can become adsorbed to the interface. The theory shows that ionic polarizability is an essential ingredient for the adsorption of chaotropic anions. The huge cost in electrostatic solvation free energy prevents adsorption of ions of low polarizability at hydrophobic interfaces. A small adsorption [11, 107] of non-polarizable ions observed in the recent classical explicit water simulations has been attributed to the artificial electrostatic surface potential of the neat air–water interface which exists in point charge water models [66]. The same artificial surface potential of classical water models was shown in the present review to lead to an excessive adsorption of the polarizable ions in the PFFMD simulations. The objective of future work should be development of classical water models with very low electrostatic surface potential. Such water models should then be compatible with the polarizable force fields and could then be used to study the interaction of ions with more complicated hydrophobic surfaces and proteins.

Acknowledgments

This work was partially supported by the CNPq, FAPERGS, INCT-FCx, and by the US-AFOSR under the grant FA9550-12-1-0438.

References

[1] Hu J H, Shi Q, Davidovits P, Worsnop D R, Zahniser M S and Kolb C E 1995 *J. Phys. Chem.* **99** 8768
[2] Knipping E M, Lakin M J, Foster K L, Jungwirth P, Tobias D J, Gerber R B, Dabdub D and Finlayson-Pitts B J 2000 *Science* **288** 301
[3] Clifford D and Donaldson D J 2007 *J. Phys. Chem.* A **111** 9809
[4] Perera L and Berkowitz M L 1991 *J. Chem. Phys.* **95** 1954
[5] Dang L X and Smith D E 1993 *J. Chem. Phys.* **99** 6950
[6] Stuart S J and Berne B J 1999 *J. Phys. Chem.* A **103** 10300
[7] Jungwirth P and Tobias D J 2001 *J. Phys. Chem.* B **105** 10468
[8] Jungwirth P and Tobias D J 2002 *J. Phys. Chem.* B **106** 6361
[9] Jungwirth P and Tobias D J 2006 *Chem. Rev.* **106** 1259
[10] Brown M A, D'Auria R, Kuo I F W, Krisch M J, Starr D E, Bluhm H, Tobias D J and Hemminger J C 2008 *Phys. Chem. Chem. Phys.* **10** 4778
[11] Horinek D, Herz A, Vrbka L, Sedlmeier F, Mamatkulov S I and Netz R R 2009 *Chem. Phys. Lett.* **479** 173
[12] Tobias D J, Jungwirth P and Parrinello M 2001 *J. Chem. Phys.* **114** 7036
[13] Kathmann S M, Kuo I F W and Mundy C J 2008 *J. Am. Chem. Soc.* **130** 16556
[14] Kathmann S M, Kuo I F W and Mundy C J 2009 *J. Am. Chem. Soc.* **131** 17522
[15] Leung K J 2010 *J. Phys. Chem. Lett.* **1** 496
[16] Weissenborn P K and Pugh R J 1996 *J. Colloid Interface Sci.* **184** 550
[17] Matubayasi N, Tsunemoto K, Sato I, Akizuki R, Morishita T, Matuzawa A and Natsukari Y 2001 *J. Colloid Interface Sci.* **243** 444
[18] Tobias D J, Stern A C, Baer M D, Levin Y and Mundy C J 2013 *Annu. Rev. Phys. Chem.* **64** 339
[19] Baer M D and Mundy C J 2011 *J. Phys. Chem. Lett.* **2** 1088
[20] Levin Y 2009 *Phys. Rev. Lett.* **102** 147803
[21] Levin Y, dos Santos A P and Diehl A 2009 *Phys. Rev. Lett.* **103** 257802
[22] Sokhan V P and Tildesley D J 1997 *Mol. Phys.* **92** 625
[23] Zakharov V V, Brodskaya E N and Laaksonen A 1997 *J. Chem. Phys.* **107** 10675
[24] Langmuir I 1917 *J. Am. Chem. Soc.* **39** 1848
[25] Wagner C 1924 *Phys. Z.* **25** 474
[26] Onsager L and Samaras N N T 1934 *J. Chem. Phys.* **2** 528
[27] Verreault D and Allen H C 2013 *Chem. Phys. Lett.* **586** 1
[28] Neyt J C, Wender A, Lachet V, Ghoufi A and Malfreyt P 2013 *Phys. Chem. Chem. Phys.* **15** 11679
[29] Moucka F, Nezbeda I and Smith W R 2013 *Mol. Simul.* **39** 1125
[30] dos Santos A P and Levin Y 2013 *Faraday Discuss.* **160** 75
[31] Geissler P L 2013 *Annu. Rev. Phys. Chem.* **64** 317
[32] Jiang N, Li P X, Wang Y L, Wang J B, Yan H K and Thomas R K 2004 *J. Phys. Chem.* B **108** 15385
[33] Romsted L S 2007 *Langmuir* **23** 414
[34] Luczak J, Markiewicz M, Thöming J, Hupka J and Jungnickel C 2011 *J. Colloid Interface Sci.* **362** 415
[35] Murgia S, Monduzzi M and Palazzo G 2012 *Langmuir* **28** 1283
[36] Müller W, Déjugnat C, Zemb T, Dufrêche J F and Diat O 2013 *J. Phys. Chem. B* **117** 1345

[37] Manet S, Karpichev Y, Dedovets D and Oda R 2013 *Langmuir* **29** 3518
[38] Lo Nostro P, Ninham B W, Pesavento A L G, Fratoni L and Baglioni P 2005 *Phys. Biol.* **2** 1
[39] Ao M and Kim D 2013 *J. Chem. Eng. Data* **58** 1529
[40] Wang W J, Sung W, Ao M, Anderson N A, Vaknin D and Kim D 2013 *J. Phys. Chem.* B **117** 13884
[41] Dawin U C, Lagerwall J P F and Giesselmann F 2009 *J. Phys. Chem.* B **113** 11414
[42] Carlton R J, Ma C D, Gupta J K and Abbott N L 2012 *Langmuir* **28** 12796
[43] Murgia S, Monduzzi M and Ninham B W 2004 *Curr. Opin. Colloid Interface Sci.* **9** 102
[44] Lopez-Leon T, Jodar-Reyes A B, Bastos-Gonzalez D and Ortega-Vinuesa J L 2003 *J. Phys. Chem.* B **107** 5696
[45] Lopez-Leon T, Santander-Ortega M J, Ortega-Vinuesa J L and Bastos-Gonzalez D 2008 *J. Phys. Chem.* C **112** 16060
[46] Peula-Garcia J M, Ortega-Vinuesa J L and Bastos-Gonzalez D 2010 *J. Phys. Chem. C* **114** 11133
[47] dos Santos A P and Levin Y 2011 *Phys. Rev. Lett.* **106** 167801
[48] Calero C, Faraudo J and Bastos-Gonzalez D 2011 *J. Am. Chem. Soc.* **133** 15025
[49] Schwierz N and Netz R R 2012 *Langmuir* **28** 3881
[50] Heydweiller A 1910 *Ann. Phys., Lpz.* **33** 145
[51] Aveyard R and Saleem S M 1976 *J. Chem. Soc. Faraday Trans. I* **72** 1609
[52] Lima E R A, de Melo B M, Baptista L T and Paredes M L L 2013 *Braz. J. Chem. Eng.* **30** 55
[53] Markovich G, Giniger R, Levin M and Cheshnovski O 1991 *J. Chem. Phys.* **95** 9416
[54] Markovich G, Pollack S, Giniger R and Cheshnovski O 1994 *J. Chem. Phys.* **101** 9344
[55] Garrett B 2004 *Science* **303** 1146
[56] Ghosal S, Hemminger JC, Bluhm H, Mun BS, Hebenstreit E L D, Ketteler G, Ogletree D F, Requejo F G and Salmeron M 2005 *Science* **307** 563
[57] Hofmeister F 1888 *Arch. Exp. Pathol. Pharmakol.* **24** 247
[58] Medda L, Barse B, Cugia F, Bostrom M, Parsons D F, Ninham B W, Monduzzi M and Salis A 2012 *Langmuir* **28** 16355
[59] Rembert K B, Paterova J, Heyda J, Hilty C, Jungwirth P and Cremer P S 2012 *J. Am. Chem. Soc.* **134** 10039
[60] Boström M, Williams D R M and Ninham B W 2001 *Langmuir* **17** 4475
[61] Manciu M and Ruckenstein E 2003 *Adv. Colloid. Interface Sci.* **105** 63
[62] dos Santos A P, Diehl A and Levin Y 2010 *Langmuir* **26** 10778
[63] dos Santos A P and Levin Y 2010 *J. Chem. Phys.* **133** 154107
[64] dos Santos A P and Levin Y 2012 *Langmuir* **28** 1304
[65] Arslanargin A and Beck T L 2012 *J. Chem. Phys.* **136** 104503
[66] Baer M D, Stern A C, Levin Y, Tobias D J and Mundy C J 2012 *J. Phys. Chem. Lett.* **3** 1565
[67] Kathmann S M, Kuo I F W, Mundy C J and Schenter G K 2011 *J. Phys. Chem.* B **115** 4369
[68] Debye P W and Hückel E 1923 *Phys. Z.* **24** 185
[69] Hansen J P and McDonald I R 1986 *Theory of Simple Liquids* 2nd edn (London: Academic)
[70] Tamashiro M N and Constantino M A 2010 *J. Phys. Chem.* B **114** 3583
[71] Rajamani S, Truskett T M and Garde S 2005 *Proc. Natl Acad. Sci. USA* **102** 9475
[72] Yaroshchuk A E 2000 *Adv. Colloid. Interface Sci.* **85** 193
[73] Levin Y and Flores-Mena J E 2001 *Europhys. Lett.* **56** 187
[74] Curtis R A and Lue L 2005 *J. Chem. Phys.* **123** 174702
[75] Buyukdagli S, Manghi M and Palmeri J 2010 *Phys. Rev.* E **81** 041601
[76] Lue L and Linse P 2011 *J. Chem. Phys.* **135** 224508
[77] dos Santos A P and Levin Y 2013 arXiv:1210.8381v2
[78] Wang R and Wang Z G 2013 arXiv:1310.8274v1
[79] Nightingale E R Jr 1959 *J. Phys. Chem.* **63** 1381
[80] Latimer W M, Pitzer K S and Slansky C M 1939 *J. Chem. Phys.* **7** 108
[81] Levin Y 2002 *Rep. Prog. Phys.* **65** 1577
[82] Diehl A, dos Santos A P and Levin Y 2012 *J. Phys.: Condens. Matter* **24** 284115
[83] Jenkins H D B and Marcus Y 1995 *Chem. Rev.* **95** 2695
[84] Marcus Y 2009 *Chem. Rev.* **109** 1346
[85] Harned H S and Owen B B 1958 *The Physical Chemistry of Electrolyte Solutions* 3rd edn (New York: Reinhold)
[86] Baer M D, Pham V T, Fulton J L, Schenter G K, Balasubramanian M and Mundy C J 2011 *J. Phys. Chem. Lett.* **2** 2650
[87] Pyper N C, Pike C G and Edwards P P 1992 *Mol. Phys.* **76** 353
[88] Matubayasi N, Matsuo H, Yamamoto K, Yamaguchi S and Matuzawa A 1999 *J. Colloid Interface Sci.* **209** 398
[89] Matubayasi N unpublished
[90] Frumkin A 1924 *Z. Phys. Chem.* **109** 34
[91] Jarvis N L and Scheiman M A 1968 *J. Phys. Chem.* **72** 74
[92] Randles J E B 1963 *Advances in Electrochemistry and Electrochemical Engineering* vol 3 (New York: Interscience)
[93] Horvath L, Beu T, Manghi M and Palmeri J 2013 *J. Chem. Phys.* **138** 154702
[94] van der Spoel D, van Maaren P J and Berendsen H J C A 1998 *J. Chem. Phys.* **108** 10220
[95] dos Santos D J V A, Müller-Plathe F and Weiss V C 2008 *J. Phys. Chem.* C **112** 19431
[96] Willard A P and Chandler D 2010 *J. Phys. Chem.* B **114** 1954
[97] Stern A C, Baer M D, Mundy C J and Tobias D J 2013 *J. Chem. Phys.* **138** 114709
[98] Randles J E B and Schiffrin D J 1966 *Trans. Faraday Soc.* **62** 2403
[99] Eigen M 1964 *Angew. Chem. Int. Edn Engl.* **3** 1
[100] Marx D, Tuckerman M E, Hutter J and Parrinello M 1999 *Nature* **397** 601
[101] Zundel G 2000 *Adv. Chem. Phys.* **111** 1
[102] Mucha M, Frigato T, Levering L M, Allen H C, Tobias D J, Dang L X and Jungwirth P 2005 *J. Phys. Chem.* B **109** 7617
[103] Petersen M K, Iyengar S S, Day T J F and Voth G A 2004 *J. Phys. Chem.* B **108** 14804
[104] Dang L X 2003 *J. Chem. Phys.* **119** 6351
[105] Petersen P and Saykally R J 2005 *J. Phys. Chem.* B **109** 7976
[106] Takahashi H, Maruyama K, Karino Y, Morita A, Nakano M, Jungwirth P and Matubayasi N 2011 *J. Phys. Chem.* B **115** 4745
[107] Netz R R and Horinek D 2012 *Annu. Rev. Phys. Chem.* **63** 401